Journal of the Korean Nuclear Society
Volume 23, Number 1, March 1991

A Study on the Pore Characteristics of the UO_2 Fuel

K-W Song, K.S. Seo, D-S Sohn, S.H. Kim, I.S. Chang
Korea Atomic Energy Research Institute
H.S. Chang
Korea Nuclear Fuel Company
(Received November 13, 1990)

UO_2 핵연료의 기공 특성에 대한 연구

송근우 · 서금석 · 손동성 · 김시환 · 장인순
한국 원자력 연구소
장홍순
한국 핵연료 주식회사
(1990. 11. 13 접수)

Abstract

The microstructure and pore characteristics have been studied on the sintered UO_2 pellet which was made of the UO_2 powder manufactured via AUC process. The open porosity decrease with the density and is nearly annihilated above the density of 10.45 g/cm^3. The round pore smaller than 3μm exist in all densities. The large and elongated pore appears additionally in low density. The pore in low density is more elongated than the pore in high density. The distribution of the pore area versus the pore size is monomodal and shows its peak on the pore size of 2 to 3μm. As the density decreases, the related area of large pore increases.

요 약

AUC 공정으로 제조된 UO_2 분말을 사용하여 소결체를 제조하여 미세 조직과 기공특성에 대하여 시험 하였다. 개기공은 소결밀도 증가에 따라서 감소하였으며, 소결밀도 10.45 g/㎤ 이상에서는 거의 소멸하였다. 3μm 보다 작은 크기의 둥근 기공이 모든 밀도에서 나타났고 낮은 밀도에서는 이것외에도 긴 기공이 관찰되었다. 같은 크기의 기공일지라도 밀도가 낮아지면 기공이 더욱 길게 나타났다. 기공크기에 따른 기공 면적의 분포는 mono 모우드이고, 2~3μm 기공크기에서 최대치를 보이는 분포를 보였다. 또한 밀도가 감소 할수록 큰 기공에 관련된 면적이 증가하였다.

1. Introduction

Experimental investigations [1,2,3,4] have shown that the irradiation behavior of nuclear fuel is dependent to a considerable extent on its pre-irradiated microstructure. Especially pore size and grain size influence the in-reactor densification and fission gas release, respectively.

The UO_2 fuel which has been fabricated in Korea is under irradiation in the Korean PWRs. In order to evaluate in-reactor fuel behavior the PIE (Post Irradiation Examination) is planned to be performed. Therefore as-fabricated properties of UO_2 fuel should be characterized.

Present work is undertaken to investigate the microstructural properties of the UO_2 fuel. The results shall be used for a comparison in the future with irradiated specimens of this type fuel.

2. Experimental

The used UO_2 powder was made via AUC(Ammonium Uranyl Carbonate) process [5]. The characteristics of UO_2 powder is shown in Table 1. Impurities of UO_2 powder were analyzed and shown in Table 2. U_3O_8 powder of 11wt% was added to UO_2 powder and homogenized completely. The homogenized powder was pressed without binder or lubricant to a green density 5.6g $/cm^3$. Green pellets were sintered at 1710℃ for about 3 hours in hydrogen atmosphere.

The sintered density and open porosity were measured by water immersion method. The pellet surface was ground prior to the measurement. The ground pellet was weighed in air. The pellet was evacuated to 0.3 Torr and then open porosity was filled with m-xylene at atmospheric pressure for about 1 hour. The impregnated pellet was weighted in air and in water. Sintered density and open porosity were calculated from the measured weights and the density of water and m-xylene [6].

Table 1 Properties of the UO_2 Powder.

Particle Size	$<100\mu m$
Apparent Density	$2.0g/cm^3$
BET-Surface	$5.0m^2/g$
O : U Ratio	2.1

Table 2 Impurities of the UO_2 Powder

Element	Content($\mu g/g$ U)
Al	160
Ca	1
F	35
Fe	<10
Mg	<1
Ni	2
Si	<7
B	<0.1
Cd	1
Cr	<2
Cu	0.4
Mn	<1
Sn	<0.6
Zn	<12

Four samples (density=10,30, 10,35, 10.40, 10.45g/cm^3) were selected, and examined ceramographically. Specimens were etched thermally and grain size were determined by linear intercept technique. Pore size distribution were obtained quantitatively using the image analyzer (Magiscan II, Joyce-Loebl Co.).

3. Analysis Methods of the Pore

Image analyzer measures characteristics of the individual pore and the measured data can be treated statistically. Pore sizes and pore shapes of specimens are determined with an aid of special software. With this program the area, perimeter, shape factor and equivalent circle diameter of each and every pore can be measured on as many measuring fields as desired.

In order to be able to intercorrelate the results the examinations should always be carried out with the same magnification and size. A magnification of 500 : 1 and a measuring field with the square 230×180 μm were used for this study. The results displayed are to be understood as two-dimensional data.

The equivalent circle diameter corresponds to the diameter of circle which has the same area as the measured object.

Equivalent diameter $=2\sqrt{(\text{area}/\pi)}$

The extent that shape of the object deviates from circle, can be represented by the shape factor.

$$\text{Shape factor}=\frac{4\pi\times\text{area}}{(\text{perimeter})^2}$$

A circle has the shape factor of 1. As the object takes a shape deviating from circle, the shape factor decreases.

4. Results and Discussion

Sintered density are in the range of 10.25g/cm^3 to 10.50g/cm^3. And most are greater than the density of 10.40g/cm^3. Fig.1 shows the open porosity as a function of the sintered density. The open porosity decreases with density and approachs nearly zero on the density greater than 10.45g/cm^3. The observed open porosity is lower than other published results[6]. This difference results mainly from higher aluminum content of this work. It is known that aluminum doping can reduce open porosity. The UO_2 powder of this work was doped with aluminum but the other work was not.

Total porosity, open porosity and closed porosity are shown schematically as a function of the sintered density in Fig.2. The open porosity falls more than the total porosity to the density of about 10.40g/cm^3 and it becomes negligible above the density of 10.45g/cm^3. On the contrary, the closed porosity increases to the density of about 10.40 g/cm^3 and then falls gradually in accordance with the decrease in the total porosity.

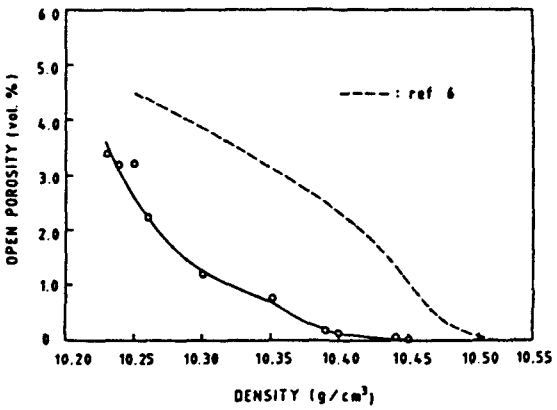

Fig.1 Dependence of the open porosity on the density

Fig. 2 indicates that open pores of about 1 vol % are changed into closed pores during densification from 10.25g/cm^3 to 10.45 g/cm^3. That can occur only if the pore exposed to surface is pinched off and becomes small and separated from the surface [7]. The pore morphology in Fig.3 seems to support this point.

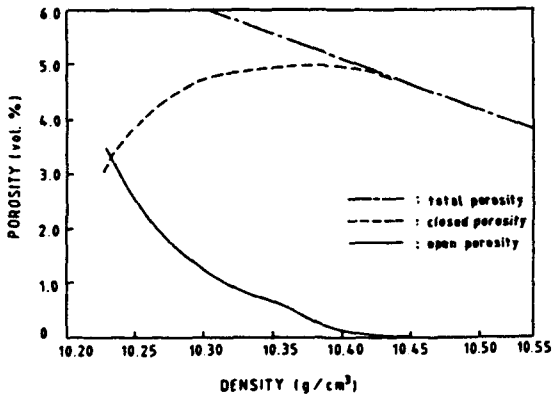

Fig.2 Dependence of the total, closed and open porosity on the density

As seen in Fig.3(a) and 3(b), elongated pores whose length are greater than 10 μm are found frequently. Nearly round pores whose diameter

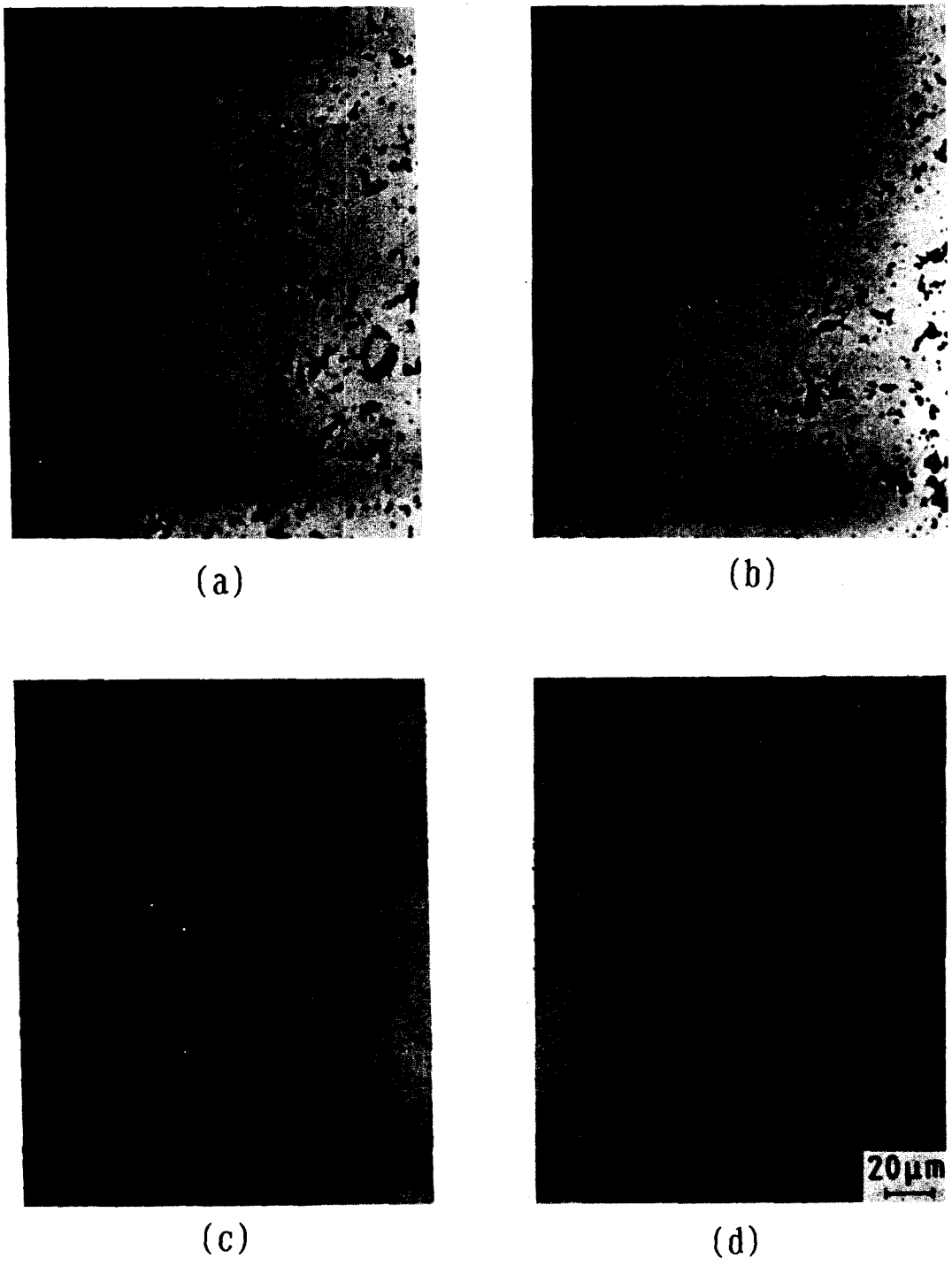

Fig.3 Photograph of pore morphology

(a) Density 10.30g/cm^3 (b) Density 10.35g/cm^3 (c) Density 10.40g/cm^3 (d) Density 10.45g/cm^3

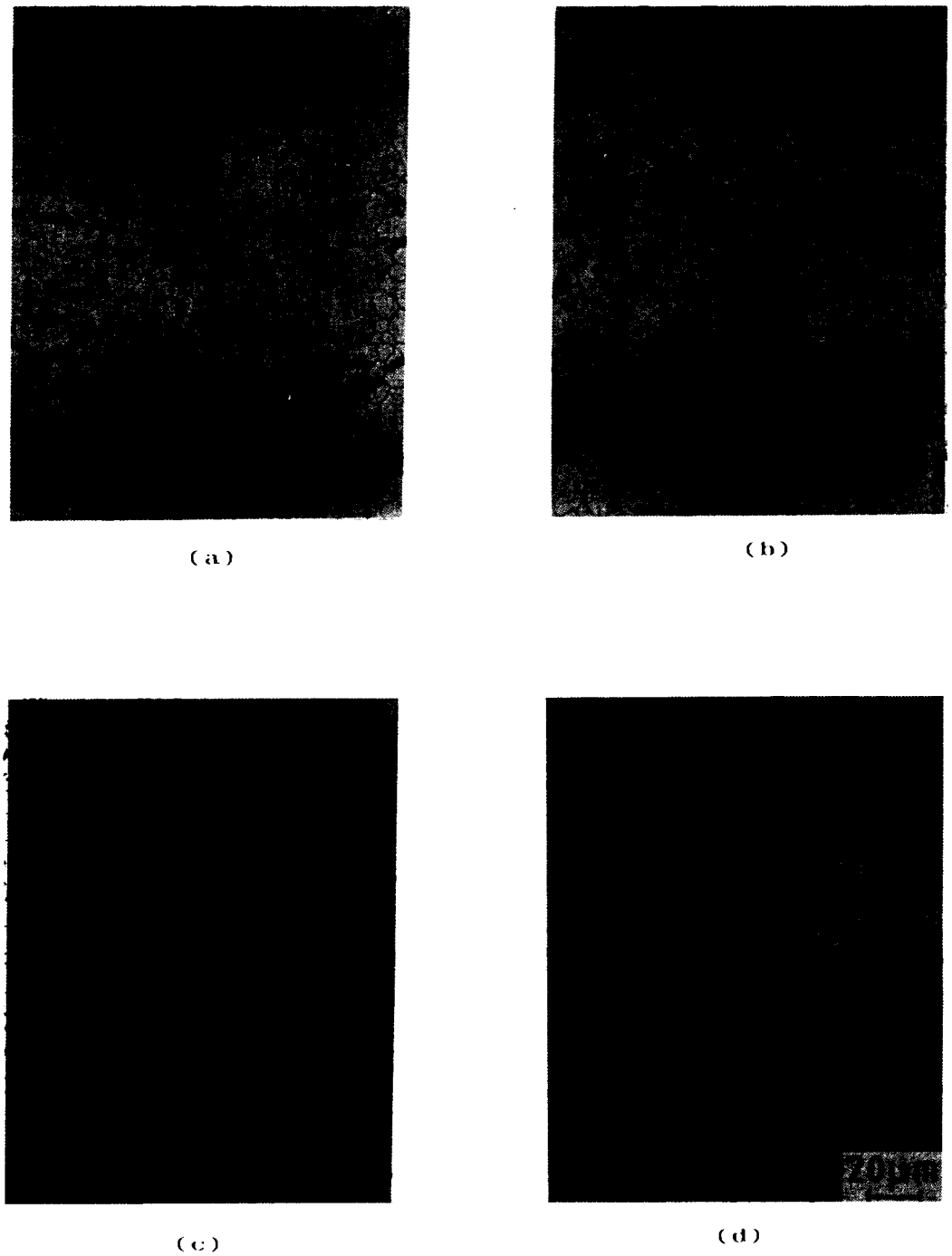

Fig.4 Photograph of grain structure

(a) Density 10.30g/cm^3 (b) Density 10.35g/cm^3 (c) Density 10.40g/cm^3 (d) Density 10.45g/cm^3

are below 3 μm are also observed. The number of elongated pores in Fig.3 (b) decreases compared with those in Fig.3(a). Fig.3(c) and Fig.3(d) show that elongated pores disappear and most pores are round and smaller than 3 μm. Consequently the elongated pore should be changed into several round pores and some pre-existing small pores should be annihilated as the density increases. The phenomena that the large and elongated pore is just pinched off can be confirmed in the photograph of 3(c) and 3(d).

The pores could be divided into three types: the round pore whose diameter is less than 3 μm, the elongated pore whose length is greater than 10 μm. Although not seen in Fig.3, the big and partly round pore lies sporadically in all densities.

Fig.4 shows the grain structure and pore morphology of the specimens. The elongated pore extending two or three grain sizes lies preferentially on the grain boundary [see Fig.4(a)]. But the round pores of about 1–3 μm which are present in all densities are not located preferentially.

The mean grain size of 9 μm is determined at the density of 10.45g/cm^3, and 8 μm at 10.40g/cm^3, and 7.6 μm at 10.35g/cm^3 and 7.2 μm at 10.30g/cm^3.

Distributions of the porosity area versus the pore size are shown in Fig.5. The porosity area represents the fraction of pore area relative to total(pore+matrix) area. Distribution is a monomodal and shows its peak on the pore size of 2 to 3 μm. The equivalent circle diameter is defined as the pore size. The pore sizes on which the pore area have maximum, are not nearly altered at the density of 10.45, 10.40 and 10.35g/cm^3. However, that pore size for 10.30g/cm^3 moved slightly to large pore size. As the density decreases, the area that the pore larger than 5 μm occupy rises gradually. The distribution are comparable to other work[8].

Fig.6 shows the dependence of the shape factor on the pore size. The shape factor of the small

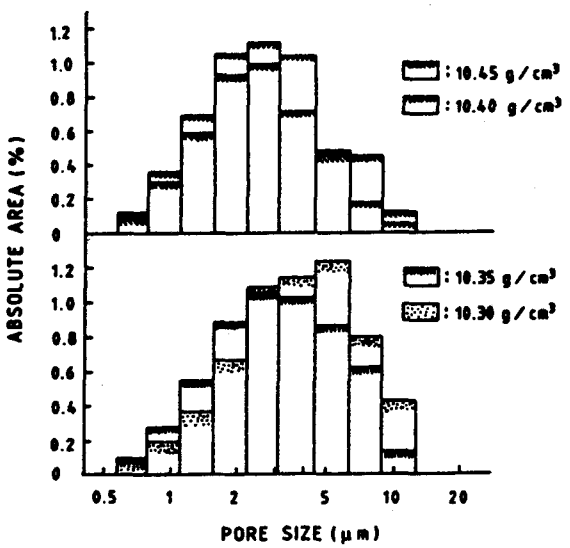

Fig.5 Pore size distribution

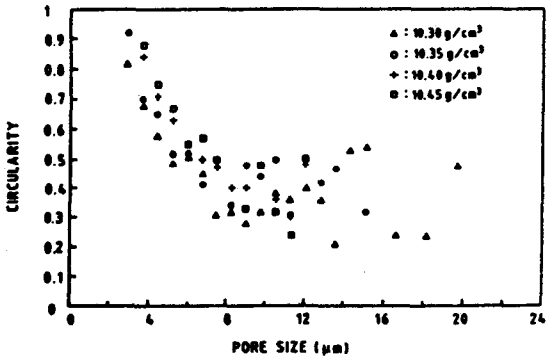

Fig.6 Dependence of the shape factor on the pore size

pore less than 2 μm could not determined, because the optical resolution was inadequate. However, the shape of that pore is shown to be nearly circular in pore morphology [see Fig.3]. The shape factor becomes small as the pore size increases. This indicates that the pores become more and more elongated. There is a tendency that the pore of lower density shows lower shape factor when the pores have the same size.

5. Conclusion

The as-fabricated characteristics of the UO_2 fuel have been studied. The open porosity decrease with the sintered density and finally annihilated on the density greater than 10.45g/cm^3. The reduction of the open porosity might be expected from the pore structure that each elongated pore is pinched off and changed into small and seperated pores during densification.

The round pore smaller than 3μm exist in all densities. In the low density, the elongated pore whose length is greater than 10μm is also appear. The elongated pores are located preferentially on the grain boundary but the round pores are located randomly. The grain sizes are in the range of 7 to 9μm.

The distribution of pore area versus pore size shows its maximum on the pore size of 2 to 3μm. The related area of large pore increases as the sintered density decreases. The pore becomes elongated as the pore size increases to 10μm.

References

1. H. Assmann and H.Stehle, J.Nucl. Mater., 81, 19(1979).
2. H. Elbel and D.Vollath, J.Nucl. Mater., 106, 243(1982).
3. G. Karsten, J.Nucl. Mater., 106, 165(1982).
4. G. Maier,H.Assmann and W.Doerr, J.Nucl. Mater., 153, 213(1988).
5. V. Mathieu, Trans. Am. Nucl. Soc., 28, 327(1978).
6. W. Doerr, H. Assmann, G.Maier and J.Steven, J.Nucl. Mater., 81, 135(1979).
7. J. Belle and B. Lustman, "Fuel Elements Conference", p.442–515 TID–7546(1958).
8. H. Assmann, W. Doerr and M. Peehs, J. Amer. Cer. Soc., 67, 631(1984).